American Journal of Applied Chemistry
2024, Vol. 12, No. 2, pp. 29-46
https://doi.org/10.11648/j.ajac.20241202.11

Research Article

Novel Biomaterial-Derived Activated Carbon from Lippia Adoensis (Var. Koseret) Leaf for Efficient Organic Pollutant Dye Removal from Water Solution

Mesele Mengesha[1], Yohannes Shuka[2, *], Tesfahun Eyoel[1], Tekalign Tesfaye[3]

[1]Department of Chemistry, Wolaita Soddo University, Wolaita Soddo, Ethiopia
[2]Department of Chemistry, Madda Walabu University, Bale Robe, Ethiopia
[3]Department of Chemistry, Mettu University, Illbabur, Ethiopia

Abstract

Today, various pollutants, such as dyes from industries, are being released into the environment worldwide, posing significant challenges that require sustainable attention and advanced solutions. This research focuses on the synthesis and characterization of a novel biomaterial-based activated carbon (AC) derived from Lippia Adoensis (Koseret) leaves and investigates its effectiveness in removing MB from aqueous solutions. The biomaterial adsorbent derived from LA was subjected to proximate analysis, pH-point zero charge (pHpzc), FT-IR, and SEM characterization. The pHpzc results indicated a slightly acidic surface functional group for AC. The impact of temperature and chemical impregnation (H_3PO_4, NaCl and NaOH) was examined, with the optimal temperature of AC preparation found to be 600 ℃. The use of H_3PO_4 for the chemical activation of biomaterials resulted in a high AC surface area. Batch adsorption experiments involved varying pH (2–10), dosage (0.1–0.35 g/50ml), initial concentration (10–35 ppm) and contact time (15–105 min). The optimal parameters were determined as pH = 8, dose = 0.25g, concentration = 10 ppm, and contact time = 75 min. The maximum adsorption capacity and removal efficiency were calculated as 3.99 and 92.2%, respectively. Thermodynamic analysis confirmed the spontaneous and endothermic nature of the system. Adsorption isotherm and kinetic studies revealed a good fit with the Langmuir isotherm (R^2= 0.999), indicating monolayer adsorption and the pseudo-second order model, respectively. These findings suggest that the use of LA-AC could offer a cost-effective solution for the removal of methylene blue from water, contributing to the solution of water pollution challenges and promoting the adoption of eco-friendly wastewater treatment technologies.

Keywords

Activated Carbon, Methylene Blue, Adsorption, *Lippia Adoensis* Leaf (Koseret), Biomaterial, Biosorbent

1. Introduction

The discharge of huge amounts of pollutants into the environment due to the rapid increase in industrial and non-industrialized activities is one of the key challenges globally [1]. Dyes are a type of pollutant that must be removed from wastewater before being released into the natural environment due to toxicity and harmful effects on photosynthetic activity

*Corresponding author: yohannesshuka@gmail.com (Yohannes Shuka)

Received: 4 April 2024; **Accepted:** 23 April 2024; **Published:** 24 May 2024

[2]. Dyes are aromatic compounds with a complex chemical arrangement that are stable under sunlight or heat and in the presence of oxidizing agents [3]. Universally, more than 10,000 different types of natural and synthetic dyes are produced yearly, balancing in the range of 7×10^5–1×10^6 tons [4].

Numerous industries, including textile, leather, paper, petroleum, printing, cosmetics, paint, rubber, plastic, food, and pharmaceuticals, produce significant amounts of toxic wastewater laden with synthetic dyes, leading to pollution due to inadequate treatment [5]. The critical characteristics of the aquatic environment are altered when textile-related toxic substances are released into the waterways. These factors include changes in pH, BOD, COD, TSS, TDS, and total suspended solids. Additionally, the water's ability to absorb light is hindered, aquatic plant photosynthesis is hampered, microbial growth is slowed, fish and other organisms are exposed to microtoxicity, and more. Above all, the carcinogenic and mutagenic nature of pollutants is detrimental to human beings [6, 7]. Additionally, the effluents of these wastes may contain various dyes, including cationic dyes, anionic dyes, and azo dyes [8].

Methylene blue (MB) is an aromatic synthetic cationic base dye commonly used in the textile industry, as an indicator and medicine [1, 9]. The dye is not considered acutely toxic, but it can have various harmful effects. Skin irritation, mouth, throat, and stomach irritation are some of the side effects of this dye's side effects; in addition, esophagus irritation, nausea, gastrointestinal pain, headache, diarrhea, vomiting, fever, dizziness, and high blood pressure are all common side effects, and they are more poisonous than anionic dyes [1, 10-12]. As a result, more studies should focus on its removal from wastewater to avoid the harmful effect on the health of living creatures.

Various treatment methods have been adopted to remove dyes from wastewater, which can be classified into physical, chemical, and biological methods [13].

Physicochemical methods have been used for the removal of various contaminants, namely solvent extraction, membrane filtration, chemical precipitation [14], photolysis [15], reduction, electrochemical treatment [16], coagulation [17], and chemical oxidation from wastewaters [18]. However, these methods have drawbacks such as high costs, high energy consumption, and many toxic by-products.

Among physicochemical methods, mainly the adsorption process assisted with carbon activation based on biomaterials is one of the most effective and economically feasible methods due to its simple operation process, low costs, easy design, high efficiency, and fast dye removal [19]. Biomaterial-based activated carbons enhance the adsorption process due to the high availability of binding sites. During this process, dye molecules are attached to the surface of a solid material (adsorbent) through physical interaction (hydrogen bonding, weak Van der Waals forces) or chemical bonding [20].

At the present time, activated carbon (AC) is the most commonly used adsorbent for dye removal because of its micropore structures, high adsorption capacity, extended surface area, and high degree of surface reactivity. Activated carbon (AC) is favored for its high efficiency in deodorization and taste removal, straightforward design, molecular-level selectivity, low energy requirements, recyclability, strong adsorption capacity, and durability in harsh conditions. Nonetheless, its widespread use is hindered by the high production costs. Economically and safely sourced organic materials, like plant leaves, are viable alternatives for creating cost-effective, biomass-based AC [21]. This is due to the fact that plant leaves are easily available and loaded with various functional groups such as alcohols, carboxylic acids, ethers, phenols, etc., which are useful in the adsorption of dye molecules [22]. Some plant-based adsorbents that have been used to remove MB from solutions include waste grape leaves [21], Neem leaves (*Azadirachta indica)* [23], Typha leaves [24], *Rubus idaeus* leaves [25]. However, there is no scientific report on the removal of MB from solution using *lippia adoensis* (LA) plant leaves adsorbent.

Lippia adoensis is one of the five indigenous species of Lippia in Ethiopia, where it occurs as an erect woody shrub up to 1-3 m tall and is a member of the family of *Verbanaceae* [26]. The plant in question is endemic to Ethiopia, thriving in altitudes between 1600-2200 meters. It exists as two varieties: the indigenous var. adoensis and the domesticated var. koseret sebsebe, commonly termed 'koseret' [27]. The latter is extensively cultivated in Ethiopia's central and southern highlands [28]. Traditionally, dried leaves are used as one of the ingredients in the preparation of spiced butter and also as a food flavoring agent and preservative. In traditional Ethiopian medicine, *Lippia Adoensis* leaves are used to treat various skin diseases such as eczema and superficial fungal infections [29]. However, despite its excellent medicinal properties, its environmental actions have not been fully explored. Our research aims to address this gap by synthesizing a new biosorbent derived AC from *Lippia Adoensis* plant leaves for the efficient removal of MB from aqueous solutions, which is a highly toxic organic pollutant dye for the ecosystem [1]. In particular, the fixed carbon yield from leaves is lower than that obtained from the stem. The study also incorporates Fourier transform infrared spectroscopy (FT-IR) and scanning electron microscopy (SEM) analyses to assess the properties of the adsorbent. Furthermore, various parameters such as contact time, initial concentration, pH, isotherm, kinetics, and thermodynamics were investigated. This biosorbent demonstrates promise in addressing water pollution challenges and in promoting the advancement of environmentally friendly technologies in wastewater treatment applications.

2. Materials and Methods

2.1. Chemicals and Reagents

Sodium thiosulfate (0.1 N), 85% H_3PO_4 (Merck), NaOH (99%, Shraddha Associates (GUJ) Pvt. Ltd., India), (KI), 0.1

M HCl, NaCl (AR grade) and Methylene blue (NICE) chemicals were used as received. The chemicals applicable for the removal of cationic dyes (Methylene blue) from waste water are of analytical grade, and distilled water was used to prepare all required solutions.

2.2. Apparatus and Equipment

The LA leaf biomaterial sample was weighed using a digital analytical balance. UV-vis measurements, conducted with a UV-VIS spectrophotometer equipped with a deuterium background corrector, were utilized to determine the absorbance of methylene blue (MB) in water samples. An electric grinder (National) was used to grind the LA leaf. The drying of the samples placed on porcelain crucibles was carried out using a drying oven (Digit heat, J. P. Selecta, Spain). pH measurement was performed using a portable pH meter (Model HI9024, HANNA Instrument). The functional groups on the activated carbon were identified using Fourier transform infrared spectrometry with a Perkin Elmer Spectrum 65 FTIR spectrometer. Surface morphology analysis of the activated carbon was conducted using a scanning electron microscope. An incubator shaker was used to agitate the conical flasks containing the samples.

2.3. Preparation of Activated Carbon

The leaves of Lippia adoensis were collected from the local area in Hawassa, Ethiopia. The collected leaves were initially washed with tap water to remove dust and subsequently rinsed with distilled water multiple times. Subsequently, the sample was air dried at room temperature (25 ℃) for a duration of 7 days. The dried sample was then crushed into granules and sieved to achieve a particle size range of (100-250) micrometers.

The raw material was impregnated with various chemicals, including H_3PO_4, NaCl and NaOH, for 24 hours with different impregnation setups. After impregnation, the carbonized samples were cooled in an inert atmosphere to room temperature, successively washed with water and 0.1 M hydrochloric acid (HCl) to eliminate residual chemical agents until achieving neutral pH in the rinsing water. The activated samples were subsequently dried at 105 ℃ for 12 hours.

Finally, activated carbon (AC) derived from Lippia adoensis leaf powder was subjected to carbonization at different temperatures ranging from 400 ℃ to 700 ℃ in a muffle furnace for a duration of 2 hours. Upon completion of the carbonization process, the material was cooled in a desiccator, crushed, and sieved to a mesh size of 200 μm to ensure consistency in the study by standardizing the particle size. The activated Lippia adoensis leaf samples treated with phosphoric acid, sodium chloride, and sodium hydroxide were labeled, respectively, as LALPA, LALSC, and LALSH for distinction *throughout the study.*

Sample storage was carried out in enclosed containers within a desiccator to maintain integrity for subsequent investigations. The schematic representation of the experimental procedure, illustrating the preparation and activation steps of activated carbon, was detailed in Figure 1 for reference.

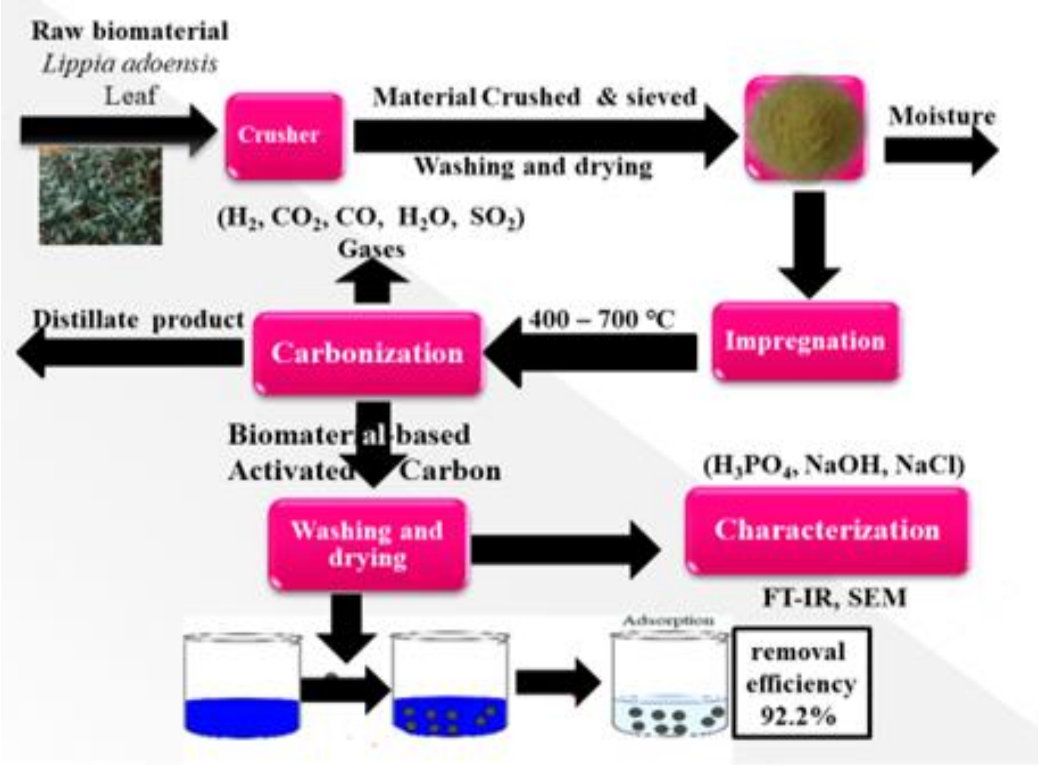

Figure 1. *The Block Diagram for the Preparation of LA-AC.*

2.3.1. Effect of Impregnation Chemical

In the investigation, the impact of impregnating Lippia adoensis biomaterial with different chemical agents - phosphoric acid (H_3PO_4), sodium chloride (NaCl) and sodium hydroxide (NaOH) - on its porous characteristics was examined. Initially, 1 gram of biomaterial was impregnated in 2 ml of each respective chemical agent (H_3PO_4, NaCl, NaOH). After thorough impregnation, the activated biomaterial was washed to eliminate excess chemicals, neutralize, and subsequent drying in a drying oven set at 105 ℃. Subsequently, the dried activated biomaterial was subjected to carbonization at varying temperatures of 400 ℃, 500 ℃, 600 ℃ and 700 ℃ to produce the activated carbon material according to the experimental setup [30].

2.3.2. Carbonization Temperature

The impact of carbonization temperature as a crucial factor in the creation of porosity during the activation process was explored. The study explored the effect of carbonization temperature on the porous characteristics of the developed activated carbon (AC) within the temperature range of 400 ℃ to 700 ℃ (specifically 400 ℃, 500 ℃, 600 ℃ and 700 ℃) for each chemical impregnation. The optimal carbonization temperature was determined based on the specific chemical utilized for impregnation, focusing on the selection of the most suitable temperature to improve the porous structure and overall performance of the activated carbon material [31].

2.4. Preparation of the Dye Solution

A stock solution of 1000 ppm methylene blue (MB) was prepared by dissolving 1 g of MB in 1 L of distilled water. To determine the dye concentration, known amounts of MB were added to distilled water to create solutions of varying concentrations. A UV/VIS spectrometer (CE1021) was used to measure the absorbance of each solution at the maximum wavelength of absorption for MB. A linear calibration curve was constructed by plotting the absorbance values against the corresponding MB concentrations. The calibration curve can be used to determine the concentration of MB in unknown samples by measuring their absorbance at the maximum wavelength and using the equation of the calibration curve to calculate the corresponding concentration.

2.5. Experimental Set-up and Removal Efficiency

For the batch experiment, 100 ml of the dye sample was placed in a 250 ml conical flask. A predetermined quantity of adsorbent was then introduced into the flask, which was agitated using a magnetic stirrer set to 200 rpm on a digital hot plate. The solution's initial pH was regulated using 1 M HCl or 1 M NaOH prior to the addition of the adsorbent. Batch adsorption experiments were performed for a wide range of temperature (25, 35, 45 and 55 ℃), contact time (15, 30, 45, 60, 75, 90, and 105 min), solution pH (2, 4, 6, 8 and 10) and adsorbent dosage (0.1, 0.15, 0.2, 0.25, 0.3 and 0.35 gram). At the end of each experiment, a small amount of the solutions was withdrawn at a predetermined time and filtered. The removal efficiency (%) and the adsorption capacity of the initial and finial concentrations of the dye at time were calculated by equations (1) and (2), respectively.

$$\text{Removal efficiency (\%)} = \frac{(Co-Ce)}{C_0}100 \quad (1)$$

$$\text{Adsorption capacity } (q_e) = \frac{(c_0-c_e)}{m}V \quad (2)$$

Where; C_0 - is initial solution concentration, C_e - is equilibrium concentration, V is the volume of the solution, m is the mass of the adsorbent

2.5.1. Effect of Adsorbent Doses

The impact of adsorbent dosage on methylene blue (MB) adsorption was investigated through a series of experiments. Initially, 50 ml of a 10 ppm MB solution was agitated with varying amounts of adsorbent (0.1, 0.15, 0.20, 0.25, 0.30, and 0.35 grams) for an optimized shaking duration, while keeping other parameters constant. Following agitation, the adsorbents were separated from the solution by centrifugation, and the remaining concentration of MB was quantified using a UV-Vis spectrophotometer (CE1021).

2.5.2. Effect of Contact Time

0.25 g of activated carbon (AC) derived from Lippia adoensis was added to conical flasks with 50 mL of 10 ppm MB solution. The flasks were placed on a laboratory shaker for various contact times (15, 30, 45, 60, 75, 90, and 105 min). The flask contents were filtered and the residual MB concentration was measured using a UV-Vis spectrophotometer (CE1021).

2.5.3. Effect of PH

The impact of pH on MB adsorption on AC of Lippia adoensis was assessed over a pH range of 2.0 to 10.0 using a portable pH meter (Model H1924, HANNA Instrument). Initially, 50 ml of 10 ppm MB solution was placed in 100 ml Erlenmeyer flasks and the pH was adjusted to the desired range (2.0-10.0) using 1 M HCl or 1 M NaOH. Subsequently, 0.25 g of AC was added and the flask contents were shaken at room temperature for the optimized duration. After filtration, the residual MB concentration was determined by UV-vis spectrophotometry (CE1021).

2.6. Isotherm Study

The equilibrium isotherms were investigated by preparing 50

ml of MB solutions at concentrations of 10 ppm, 15 ppm, 20 ppm, 25 ppm, 30 ppm and 35 ppm in 100 ml Erlenmeyer flasks. Subsequently, 0.25 g of Louisiana leaf powder activated carbon (AC) was added to each solution, followed by agitation in a laboratory shaker. The contents of the flasks were then filtered, and the concentration of MB in the solution was quantified using a UV-vis spectrophotometer (CE1021). To determine the adsorption capacity of the adsorbent, the experimental data obtained were analyzed by fitting them against the Langmuir and Freundlich isotherm equations [32].

2.7. Kinetic Study

The kinetic study was initiated by preparing 50 ml of a Methylene Blue (MB) solution with an initial concentration of 10 ppm in 100 ml Erlenmeyer flasks. Subsequently, 0.25 g of Louisiana leaf powder activated carbon (AC) (LA) was introduced into the solution. Sampling was carried out at specific time intervals (15, 30, 45, 60, 75, 90, and 105 min), and the concentration of the filtrate was determined using a UV-Vis spectrophotometer (CE1021). The obtained experimental data were then subjected to analysis against kinetic models to elucidate the underlying mechanisms of the adsorption processes. The kinetic adsorption behavior on AC of LA was evaluated by fitting the data to both pseudo first-order and pseudo second-order kinetic models as outlined in reference [33].

2.8. Thermodynamic Study

Determination of the basic thermodynamic parameters; enthalpy of adsorption (ΔH^o), Gibb's free energy of adsorption (ΔG^o) and entropy of adsorption (ΔS^o), is to analyze the process from a thermodynamic point of view. These are used to assess the spontaneity and nature (exothermic or endothermic) of the process [34].

A thermodynamic study was conducted to investigate the adsorption behavior of Methylene Blue (MB) in powder activated carbon (AC) from Louisiana leaf powder. Initially, 50 ml of MB solutions with an initial concentration of 10 ppm were prepared in 100 ml Erlenmeyer flasks. Subsequently, 0.25 g of LA AC was added to each solution. The solutions were then subjected to agitation at various temperatures (25 ℃, 35 ℃, 45 ℃ and 55 ℃). After agitation, the contents of the flasks were filtered and the concentration of MB in the filtrate was determined using a UV-Vis spectrophotometer (CE1021). This experimental procedure was carried out to investigate the thermodynamic aspects of the adsorption process between MB and LA AC.

2.9. Performance Analysis

2.9.1. Iodine Number

The iodine number is a metric that quantifies the milligrams of iodine that can be absorbed by 1 gram of activated carbon. It serves as a reliable estimate of the surface area and microporosity of the carbon material. To determine the iodine number, we adhere to the American Society of Testing and Materials (ASTM) protocol, employing the sodium thiosulfate ($Na_2S_2O_3$) volumetric technique. This involves blending activated carbon with a 0.02 N iodine solution, intermittently shaking the mixture, followed by titration against $Na_2S_2O_3$. The outcome provides the adsorption capacity of the carbon, denoted in mg/g. [35]. In practice, 0.25 grams of activated carbon is treated with a standard iodine solution under controlled conditions. The carbon is then processed with 10.0 ml of 5% HCl, boiled for 30 seconds, and allowed to cool. Subsequently, 100 ml of 0.1 N iodine solution is introduced and stirred for 30 seconds. After filtration, 50 ml of the filtrate is titrated with 0.1 N sodium thiosulfate using starch as an indicator. The adsorption data, represented as the ratio of adsorbed iodine to carbon weight (X/M), is plotted against the iodine concentration in the filtrate on logarithmic scales. Should the residual iodine concentration fall outside the 0.008 to 0.04 N range, the experiment is repeated with varying amounts of carbon for each data point. The iodine number is then defined as the amount of iodine adsorbed at a residual concentration of 0.02 N, expressed in mg/g. The X/M and C values are calculated by equations (3) and (4), respectively.

$$\frac{X}{M}\left(\frac{mg}{g}\right) = \left\{\frac{\left(N_{1*126.93*V_1}\right) - \frac{[V_1+V_{HCl}]}{V_F}*\left(N_{Na_2S_2O_3}*126.93\right)V_{Na_2S_2O_3}}{M_C}\right\} \quad (3)$$

$$C = N_{Na_2S_2O_3} * \frac{V_{Na_2S_2O_3}}{V_F} \quad (4)$$

Where; N_1 - is the normality of the iodine solution

V1 is the added volume of the iodine solution.

HCl is the added volume of 5% HCl.

VF is the filtrate volume used in a titration, N is the sodium thiosulfate solution, normality is the volume consumed of sodium thiosulfate solution, and M is the mass of activated carbon.

2.9.2. Methylene Blue Number

The Methylene Blue Number (MBN) serves as an indicator of the mesoporosity within activated carbon (AC), specifically the pores ranging from 2 to 5 nm. It is quantified as the maximal volume of dye that can be adsorbed by 1.0 gram of the adsorbent material. During the testing process, 10.0 milligrams of AC are combined with 10.0 milliliters of methylene blue at varying concentrations (10, 25, 50, 100, 250, 500, and 1000 mg/L) and left to interact for 24 hours at a standard room temperature of about 25 ℃. Post-interaction, the residual concentration of methylene blue is determined with the aid of a UV/Vis spectrophotometer [36]. The quantity of dye each sample of AC adsorbs is then computed using Equation (5);

$$MBN\left(\frac{mg}{g}\right) = \frac{(Co-Ce)}{M}V \quad (5)$$

Where; C_0 - (mg L^{-1}) is the concentration of the methylene blue solution at starting time (t = 0), Ce - (mg L^{-1}) is the concentration of the methylene blue solution at equilibrium time, V (L) is the volume of the treated solution and M (g) is the mass of the adsorbent.

2.9.3. Moisture Content

The moisture content was determined by the loss on drying method. 2500 mg of equally grinded LA leaf powder (carbonized and uncarbonized) was accurately weighted and placed in a clean crucible of a known weight. Then the crucibles were placed in an oven at 105 ℃ to a constant weight. After 7 h, the weight of the LA leaf powder (carbonized and non-carbonized) and the crucible was weighted and finally, the moisture content was calculated using equation (6) as expressed by [37];

$$\text{MC } (\%) = \frac{WB - WA}{WB} \times 100\% \quad (6)$$

Where; MC is the moisture content of the LA leaf powder (carbonized and uncarbonized) in percentage, WB is the weight of the sample before drying and WA is the weight of the sample after drying.

2.9.4. Ash Content

The ash content of the LA leaf powder (carbonized and uncarbonized) was determined by weighting 2500 mg of LA leaf powder (carbonized and uncarbonized) and placed in a dried crucible. The crucibles containing the sample were put in a muffle furnace at a temperature of 500 ℃ for 2.00 hours. Finally, the crucibles removed from the furnace and the LA leaf powder sample (carbonized and uncarbonized) were weighed and the percent of the ash content calculated using the following equation (7);

$$\text{AC } (\%) = \frac{WB - WA}{WB} \times 100 \quad (7)$$

Where; AC is the ash content in percent, WB is the weight of the LA leaf powder sample (carbonized and uncarbonized) before heating, and WA is the weight of the LA leaf powder carbonized and uncarbonized sample after heating.

2.9.5. Volatile Matter

With little modification to the method described by [38]; 2.5 g of LA leaf powder (carbonized and uncarbonized) was taken and placed in a dried crucible and heated in a muffle furnace adjusted at 700 ℃ for 8 min. Then the crucibles were cooled and weighed. Finally, the volatile matter of the LA leaf powder (carbonized and uncarbonized) was calculated using the following equation (8);

$$\text{VM} = \frac{\text{WB} - \text{WA}}{\text{WB}} \times 100 \quad (8)$$

Where: VM (volatile matter of the LA leaf powder (carbonized and uncarbonized) in percentage), WB is (weight of the LA leaf powder (carbonized and uncarbonized) sample before heating), and WA is (weight of the sample after heating).

2.9.6. Fixed Carbon Content

Fixed carbon is a calculated value that results from the summation of the percentages of moisture, ash, and volatile matter subtracted from 100, as shown in Equation (9);

Fixed carbon, % = 100 – (moisture, % + ash, % + volatile matter, %)

$$\% \text{ FC} = 100 - (\text{MC} + \text{VM} + \text{AC}) \quad (9)$$

The yield of activated carbon (AC) was calculated on a chemical-free basis and can be regarded as an indicator of the process efficiency for the chemical activation process. The AC yield is calculated as the percentage weight of the resultant activated carbon divided by the weight of dried *Lippia Adoensis* as shown in Equation (10);

$$Y_{AC} = \frac{W_{AC}}{W_{LA}} \times 100\% \quad (10)$$

Where: W_{AC}, = weight of activated carbon, W_{LA} = uncarbonized sample of *Lippia Adoensis* leaf powder uncarbonized sample respectively

2.9.7. Determination of the Point of Zero Charge

The pH at the point of zero charge (PZC) is defined as the pH value at which a material's surface bears no net electrical charge under specific conditions of temperature, pressure, and composition of the aqueous solution. It's important to note that at the pH of PZC, the surface is not devoid of charge; rather, it possesses equal quantities of negative and positive charges. Three distinct types of zero-charge points are recognized: the point of zero charge, the point of zero net proton charge, and the point of zero net charge. The point of zero charge is also known as the isoelectric point, where particles remain stationary in an electric field.

To ascertain the pH_PZC, the salt addition method is employed. This involves mixing 0.25 grams of the adsorbent with 30 milliliters of a 0.01 mol/L NaCl solution at various pH levels. The pH is adjusted between 2 and 10 using either 0.1 mol/L HCl or 0.1 mol/L NaOH, and this initial pH is recorded. After a period of 24 hours, the final pH is measured with a pH meter. The change in pH (ΔpH) is plotted on the y-axis against the initial pH (pHi) on the x-axis. The pH_PZC is identified at the point where the curve intersects the x-axis [3].

2.10. Characterization

FT-IR analysis was used to characterize the functional groups on the surface of the prepared activated carbon before and after adsorption. The FTIR study identified organic and

inorganic groups involved in the adsorption process by observing changes in frequency. The activated carbon samples were scanned for functional groups using FTIR in the range of 400-4000 cm^{-1}. In addition, scanning electron microscopy (SEM) was utilized to visualize the porous structure of the activated carbon sample treated with H_3PO_4.

3. Results and Discussions

3.1. Optimization of Carbonization Temperature and Impregnation Chemicals

The impact of carbonization on the adsorption capacity of activated carbon (AC) is illustrated in Figure 3. As the temperature increased from 400 to 600 ℃, the adsorption capacity (% removal efficiency) of AC derived from LA increased, peaking at 600 ℃ before irregularly declining with further temperature increases. The decline in adsorption capacity at higher temperatures may be attributed to reduced pore volume and surface area, or the degradation of AC at elevated temperatures. The analysis of Figure 2a and Table S1 indicates that the optimal carbonization temperature for the activated carbon derived from LA was 600 ℃. Furthermore, the influence of impregnation chemicals on the performance of microporous ACs is depicted in Figure 2b. AC produced from LA by impregnation with H_3PO_4 exhibited the highest adsorption capacity.

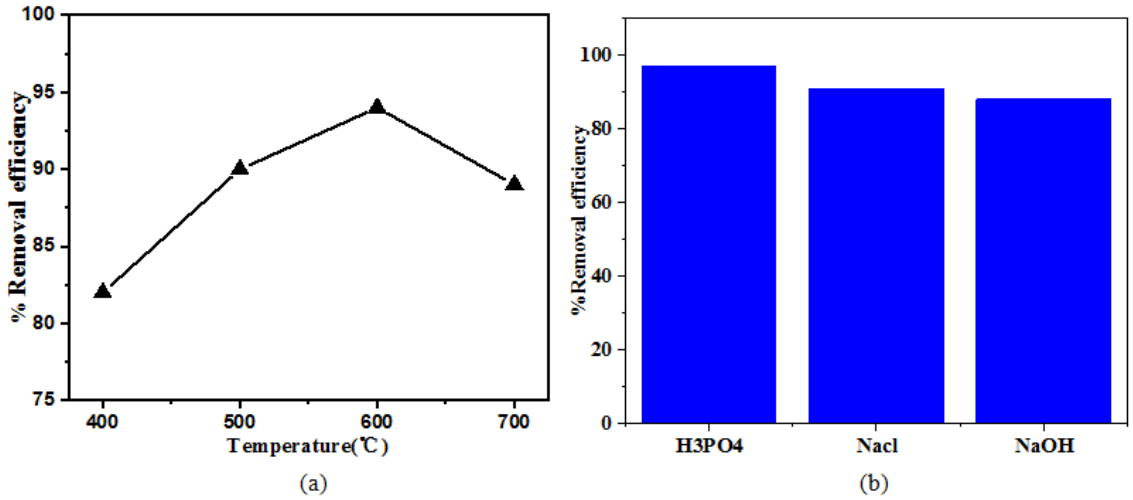

Figure 2. *The Effect of Carbonization Temperature (a) and Active Reagents (b) on the Preparation of AC from LA.*

3.2. Characterization of the Prepared Activated Carbon

3.2.1. Iodine Number and Methylene Blue Number

The iodine number is an essential metric for assessing activated carbon's efficacy. It gauges the micropore content within the carbon, determined through the carbon's capacity to adsorb iodine from a solution. The mesopores, which form during the carbon's activation, account for its expansive surface area and are the primary sites for adsorption. The higher the iodine number, the greater the sorption capacity [39].

In Figure 3, we observed that the activated carbon iodine number of LA shows a direct proportionality with the microporosity of the sample, thus a higher iodine number signifies a higher microporosity of the sample. It was observed that the iodine number of AC of LA was the highest value and its value was calculated using the equation. (3) to be 605 mg/g.

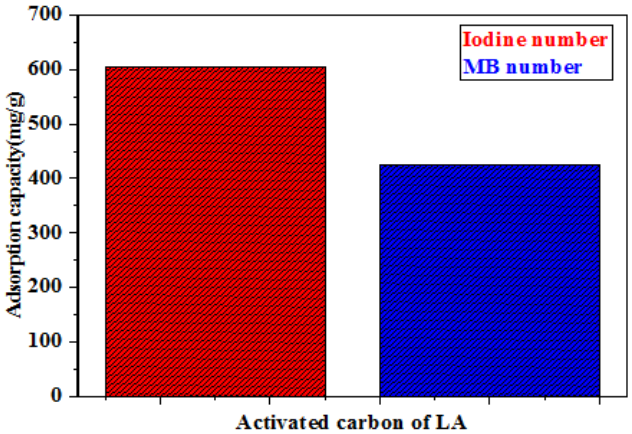

Figure 3. *Adsorption of Iodine number and Methylene blue number.*

The methylene blue value was utilized to assess the surface area and pore size distribution of the activated carbon derived from Louisiana leaf powder. This value signifies the adsorp-

tion capacity of activated carbon for molecules similar in size to methylene blue, as well as the surface area resulting from the presence of pores larger than 1.5 nm. The calculated value of methylene blue using Equation (5) was determined to be 424 mg/g. In Figure 3, it is observed that for Louisiana activated carbon, the adsorption capacity based on the iodine number was maximized compared to the value of methylene blue.

3.2.2. Proximate Analysis of LA and LA Activated Carbon

The exact analysis results of the LA sample before the activation process is carried out in order to know the moisture content, the ash content, the volatile matter and the carbon content using the muffle furnace in the physical chemistry laboratory of Hawassa University physical chemistry lab according to the American Society for Testing Materials and the result is shown in Table 1 below.

Table 1. *Proximate analysis of uncarbonized LA leaf powder and uncarbonized LA leaf powder by phosphoric acid.*

Proximate analysis (%)				
Sample	**Moisture Content**	**Volatile Matter**	**Fixed carbon Content**	**Ash Content**
*UC-LA	3.6	54	26.3	16.1
*C-LA	2.7	20.2	54.9	22.2

*UC-LA = Uncarbonized LA Sample, C-LA = Carbonized LA

As shown in table above, a small amount of moisture and ash content is better for chemical treatment because the sample with a higher moisture content needs more heat to evaporate the moisture. A high ash content also affects the chemical treatment, which would reduce the overall activity of the adsorbent. This implies that the lower the ash content, the better material for chemical treatment [40]. As the moisture content is lower, the effectiveness of the adsorbent increases; this is because water molecules would have the potential effect of filling the adsorbent binding site before it contacts the solution (adsorbate); this reduces the efficiency of the activated carbon. Therefore, the prepared activated carbon produced was stored in an air tight bag; otherwise, it could adsorb the moisture content from the environment [37]. Proximate analysis of LA treated raw and phosphoric acid treated LA activated carbon; Difference estimated after the activation process, the volatile matter content decreased significantly, whereas the fixed carbon content increased in the activated sample. This is because most of the organic substances have been degraded and discharged both as gas and liquid tars, leaving a material with high carbon purity. Generally, the lower the ash value, the better activated carbon for use as an adsorbent [37].

3.2.3. pH Point of Zero Charge (pHpzc)

The pHpzc values for the activated carbon LA were 6. The pHpzc value at 6 indicates that the LA surface has the presence of acid functional groups. Furthermore, pH <6, implies the values of pH < 6, implies that the dominancy of acidic functional groups compared to the basic ones. The positive charge on the surface of the LA could be obtained at a pH below the pHpzc value, and the negative charge on the surface of the LA could be obtained at pH levels above the pHpzc value. A positive charge of LA is favorable to the uptake of negative-charge (anionic) species; on the other hand, a negative charge of LA is favorable to the uptake of positive-charge (cationic) species. During the study of the adsorption test, investigation of the pHpzc value would help to select the pH value of the medium. Hence, the percent adsorbent removal capacity increased below and above the pHpzc value for anionic and cationic species [41]. Figure 4 and Table S3 show that the point of zero charge (pHpzc) of the activated carbon derived from the LA leaf was 6 and at this point the surface of LA is neutral but below and above this point the surface of LA is positively and negatively charged, respectively, which attracts the positively charged methylene blue ion and this results in an increase in adsorption.

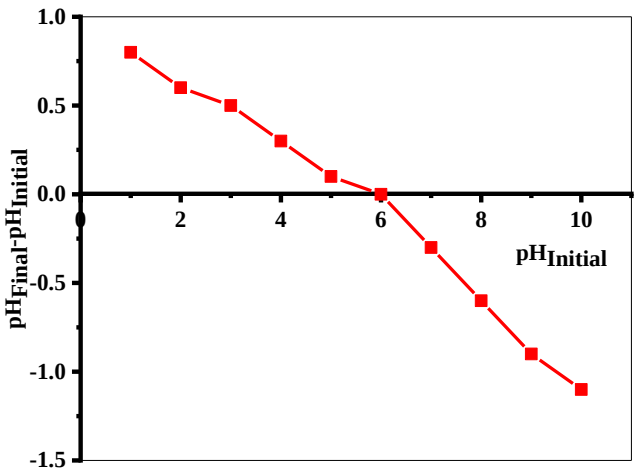

Figure 4. *The pH on point zero charge of AC of LA.*

3.2.4. FT-IR Analysis

Various absorption bands within the 4000–400 cm^{-1} range were recorded in the FT-IR spectra of activated carbon prepared from LA leaf as shown in Figure 5. The FT-IR spectrum of LA leaf AC shows that some distinct changes are observed between the spectra before and after adsorption. The increase in intensity and shift in peak positions in LA after MB biosorption demonstrate the involvement of different functional groups during the adsorption. Before adsorption of the MB ion, there was a peak formation at a wave number 2930, 2860, 1654, 1464, 1376 and 726 cm^{-1}. After MB adsorption, the peaks shifted to 2926, 2856, 1648, 1464, 1378, and 726 cm^{-1} but also there is a remarkable change of the intensities of infrared bands with no change positions. These changes in wave number show that the hydroxyl, alkane, and aromatic groups are involved in the adsorption of MB ions. Therefore, the functional groups of the C=C, C-C, and –CH groups in the LA leaf would participate to interact with the MB ion, involving the mechanism of surface complex, hydrogen bonding, and electrostatic attraction. These may result from an interaction between the positive centers of the MB dye and the negative centers of the LA adsorbent, which involves significant attractive forces. The presence of adsorbed water molecules is supported by the absorption band located at 1654 cm^{-1} commonly assigned to bending vibration of the adsorbed water molecule [42].

Bands indicates at 2930 cm^{-1} is C-H stretching of alkane and bands arising in the stretching vibration mode at 1464 cm^{-1} is C=C- bond in aromatic compounds [43, 44]. We can conclude that the two spectra are similar in their features, which indicate their very close chemical composition and nature, but may be different in concentration.

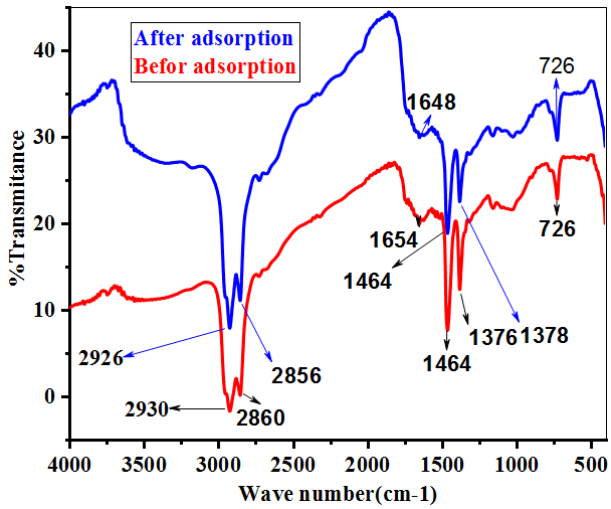

Figure 5. *FTIR spectrum of LA-AC before & after adsorption.*

3.2.5. SEM Analysis

SEM images of the LA sample before and after adsorption of the MB dye are shown in Figures 6a and 6b, respectively. The prepared AC was examined by Scanning Electron Microscope to analyze the surface of the adsorbents. The SEM of chemically activated carbons by H_3PO_4 after adsorption is presented in Figure 6b. The activated carbon of LA prior to adsorption was well-developed, and a porous surface was observed at higher magnification than the activated carbon of LA. The pores observed from SEM images have diameters in the micrometer (μm) range.

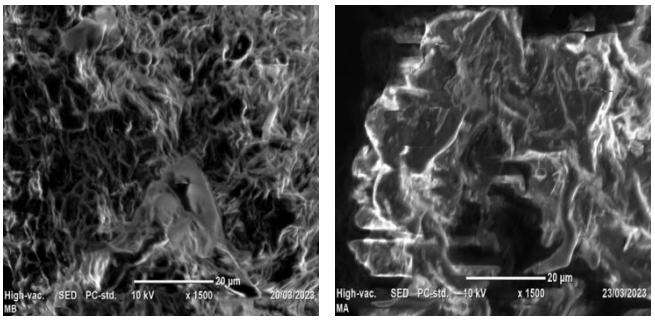

a) Before adsorption b) after adsorption

Figure 6. *SEM images of LA-AC before and after adsorption.*

From Figure 6a, the forms and shapes of the particles are irregular and their surface is rough and porous. The distribution of particle sizes is not uniform. It was observed that the pore size reduces after adsorption. This indicates that LA is effective in adsorbing methylene blue.

3.3. Batch Adsorption Study

3.3.1. Calibration Curve Plotted for Methylene Blue Adsorption

The calibration curve plotted for methylene blue at a wavelength of 665 nm was obtained from standard solutions of methylene blue with different concentrations and the corresponding absorbance (Figure 7). It is important to determine the unknown concentration of MB.

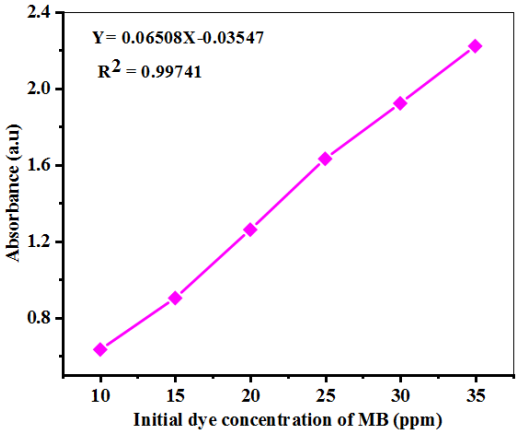

Figure 7. *Calibration curve for methylene blue solution.*

3.3.2. Effect of Adsorbent Dose

In the dosage study conducted within the realm of adsorption studies, the objective of the experiment was to determine the adsorbent capacity concerning a specific initial concentration of dye present in a solution. Using typical dye solutions of 10 ppm derived from the stock solution, varying amounts of adsorbent ranging from 0.1 g to 0.35 g were introduced to each solution. The impact of the dose of the adsorbent on the efficiency of the removal of Methylene Blue (MB) using activated carbon (AC) from LA is depicted in Figure 8. In particular, the removal efficiency of MB by AC of LA increased from 66.1% to 92.2% as AC doses increased from 0.1 g to 0.25 g per 50 ml of solution, maintaining a fixed MB concentration of 10 ppm.

However, it was observed that the adsorption capacity demonstrated a decrease, as it is inversely proportional to the mass of the adsorbent. This phenomenon can be attributed to the increase in the adsorbent surface area and the availability of additional adsorption sites resulting from the heightened adsorbent dosage. At elevated dosages of the adsorbent, equilibrium in adsorption was quickly achieved due to osmotic pressure, despite the presence of unused active sites, in contrast to lower dosages of the adsorbent, leading to more efficient utilization of adsorption sites [45].

On the contrary, at lower doses of the adsorbent, particularly when employed in higher-concentration MB solutions, the adsorbent exhibited a tendency to saturate rapidly, resulting in a diminished adsorption removal capacity. Subsequent to extensive experimentation, a median dose of 0.25 g was identified as the optimal point for subsequent adsorption experiments due to its favorable performance characteristics.

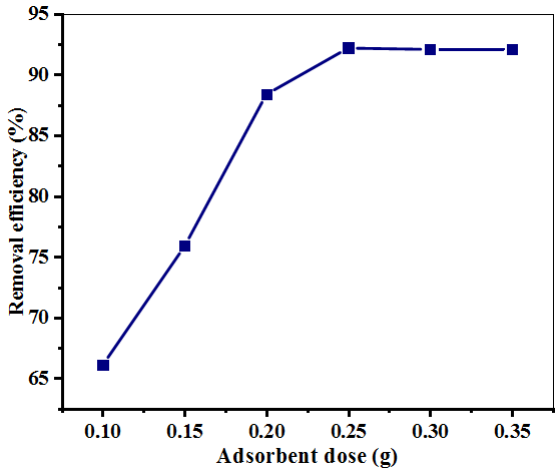

Figure 8. *Effect of the adsorbent dose on the preparation of AC of LA.*

3.3.3. Effect of Initial Dye Concentration

In this study, 0.25 g of LA powder was added to 50 ml solutions with varying concentrations (ranging from 10-35 ppm) of typical dye solutions at pH 8, which were prepared by dilution for use as functional solutions. The impact of initial concentration on the efficiency of MB removal was investigated using AC of LA, and the results are presented in Figure 9 and Table S5. The MB removal efficiency of LA AC was observed to decrease from 94.5% to 55%. This decrease can be attributed to a reduction in the surface area of the adsorbent and the availability of fewer adsorption sites due to the constant dosage of the adsorbent [46]. In addition, a higher adsorption capacity was found at higher initial dye concentrations [47]. Therefore, the optimal point for the initial concentration of MB removal was determined to be 94.5%.

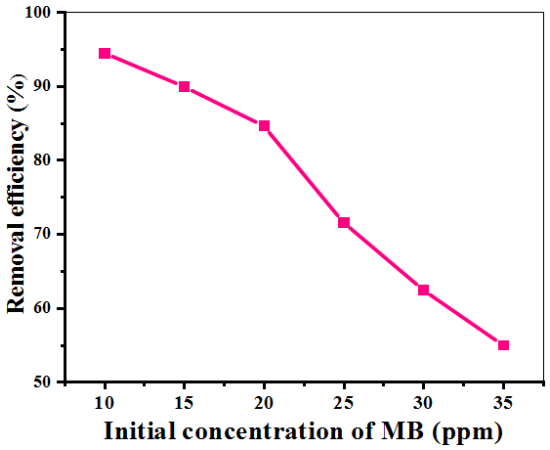

Figure 9. *Effect of Initial Concentration on the Preparation of AC of LA.*

3.3.4. Effect of pH

An investigation into the impact of pH on adsorption can be conducted by preparing a solution of adsorbent and adsorbate with a constant adsorbent amount and dye concentration, but varying the pH by adding 1 M NaOH or 1 M HCl solutions, followed by agitation until equilibrium is reached. Typically, at lower pH levels, there is a reduction in the removal efficiency for cationic dyes, whereas anionic dyes exhibit increased removal rates. Conversely, at higher pH levels, the removal efficiency for cationic dyes improves, while it diminishes for anionic dyes. This is because, at elevated pH, the solution interface's positive charge diminishes, rendering the adsorbent surface negatively charged, which in turn boosts cationic dye adsorption and reduces anionic dye adsorption. On the other hand, at lower pH levels, the solution interface's positive charge intensifies, causing the adsorbent surface to become positively charged, which enhances anionic dye adsorption and lowers cationic dye adsorption [48]. In this study, the effect of pH on the adsorption of MB on AC was examined in the pH range of 2-10. Figure 10 and Table S6 represent the effect of on the adsorption of MB. The AC of LA showed an optimal value at pH 8 (92.93%) and decreases with increasing and decreasing value. These values indicate that activated carbon of LA is applicable for the removal of MB from aqueous solution under basic media [49].

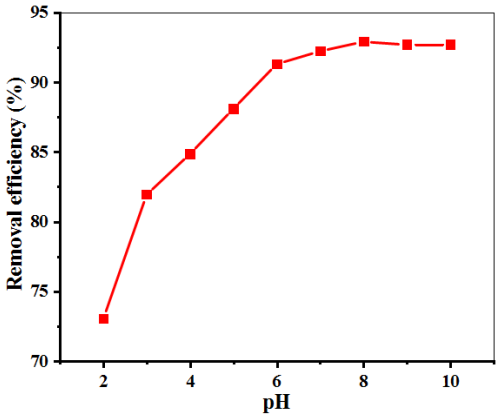

Figure 10. *Effect of pH on the Preparation of AC of LA.*

3.3.5. Effect of Contact Time and Temperature

To find the time for equilibrium adsorption, the contact time of MB in LA was varied from 15 min to 105 min at a fixed MB concentration of 10 ppm, a dosage of 0.25 g per 50 ml solution, at 25 ^{0}C. The presence of a large number of vacancies on the adsorbent surface that reached saturation at equilibrium is believed to be responsible for the sharp increase in the adsorption capacity at the initial contact time. Due to the lack of active sites for dye biosorption once equilibrium was established, it remains nearly constant [50]. Adsorption reaches maximum, 92.4% for LA activated at 75 min Figure 11a and Table S7. Hence, the optimum contact time for activated carbon of LA was selected as 75 min for further experiments. Figure 11b and Table S8 show that the increase in temperature leads to the increase in both adsorption efficiency and capacity. The adsorption is an endothermic process; as the temperature increases, the adsorption equilibrium shifts directly or the concentration of the adsorbent in the solution is increased, leading to an increase in the adsorption efficiency and capacity. This may be due to the fact that at higher temperatures the solute molecules show an inclination to escape from the solid phase and reenter the liquid phase due to increased mobility [51].

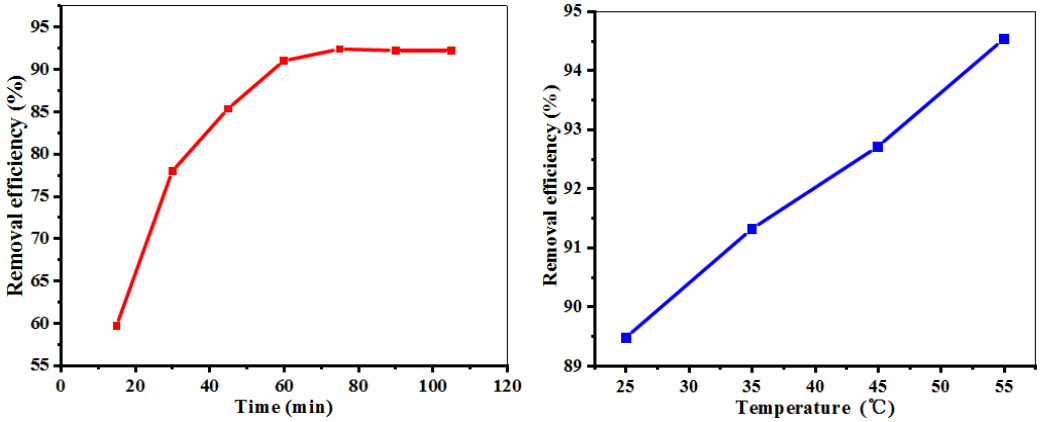

(a) (b)

Figure 11. *Effect of contact time (a) and temperature (b) on the removal of MB for AC of LA.*

3.4. Adsorption Thermodynamic Study

Standard changes in Gibbs free energy (ΔG^0), entropy (ΔS^0), and enthalpy (ΔH^0) are key thermodynamic parameters that help to understand the adsorption behavior of Methylene blue in adsorbents [52]. The uptake of MB on LA is also analyzed with reference to the changes that occurred in the thermodynamic parameters according to Eq. (1) and the values are presented in Table S7. From Eq. (1) ΔH^0 and ΔS^0 were obtained from the slope of the lnKc plot compared to 1/T Figure 12 and Table S9-10. The negative values of ΔG^0 at 298, 308, 318 and 328 K revealed that MB uptake in LA was spontaneous. Similarly, the positive value of H0 revealed that uptake was endothermic. This could be assigned to hydrogen bond formation between MB and LA. The positive ΔS^0 value for the chosen system is due to the improved randomness at the MB-LA solution interface [53].

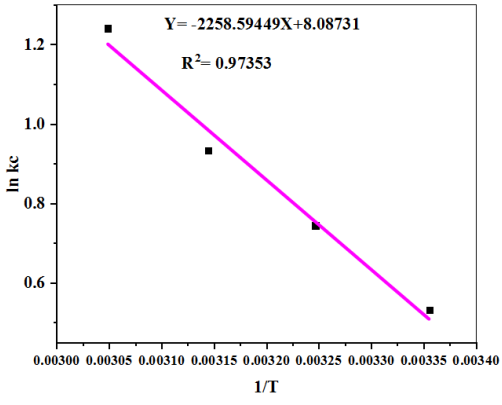

Figure 12. *Vant Hoff plot for determination of the thermodynamic parameter for the adsorption of MB.*

3.5. Adsorption Equilibrium Study

In this study, adsorption equilibrium is reached when the amount of adsorbed solute equals the amount desorbed. Equilibrium adsorption isotherms depicting solid phase concentration (qe) against liquid phase concentration (Ce) of the solute were utilized. These isotherms provide information on the adsorption capacity of the adsorbent, solute-solution interactions, and adsorbate accumulation on the adsorbent surface [54]. The adsorption of Methylene blue on the prepared activated carbon was investigated using Langmuir and Freundlich isotherm models, as detailed in Table S10.

3.5.1. Langmuir Isotherms

The Langmuir model assumes that adsorption occurs on a homogenous surface by monolayer adsorption and that there is no interaction between the adsorbed molecules. The linear form of the model is expressed in Eq. (11);

$$\frac{c_e}{q_e}=\frac{1}{q_{max}}.c_e + \frac{1}{q_{max}.K_l} \quad (11)$$

Where C_e is the equilibrium concentration (mg•L^{-1}), q_e the amount adsorbed at equilibrium (mg•g^{-1}), q_{max} is the maximum monolayer adsorption capacity of the adsorbent, and KL is the Langmuir constant related to the adsorption capacity and the energy of adsorption. The linear plot of c_e/q_e versus c_e gives a straight line and q_{max} and K_L are determined from the slope and intercept of the plot, respectively (Figure 13a). To determine the favorability of the adsorption using this model, a dimensionless separation factor was calculated, given as Eq. (5). Based on the correlation coefficients (R^2), it is clear that the adsorption of MB on activated carbon is best fitted to the Langmuir adsorption isotherm for the entire range of concentrations. From Table 2 the value of R^2 more approaches to 1 indicates the fact that the Langmuir isotherm fits the experimental data very well and may be due to the homogenous distribution of active sites on the carbon surface, since the Langmuir equation assumes that the surface is homogeneous.

3.5.2. Freundlich Isotherms

For the Freundlich model, the adsorption takes place on a heterogeneous surface by multilayer adsorption. The model is expressed linearly in Eq. (12);

$$logq_e = logK_L + \frac{1}{n}logc_e \quad (12)$$

where KF (mg/g) (mg/L) and n are the Freundlich constants related to the adsorption capacity and the adsorption intensity, respectively. The KF and n values were calculated from the intercept and slope of the $logq_e$ versus log ce plots Figure 13b. If the value of n is greater than one, this indicates a good adsorption of MB onto the adsorbent.

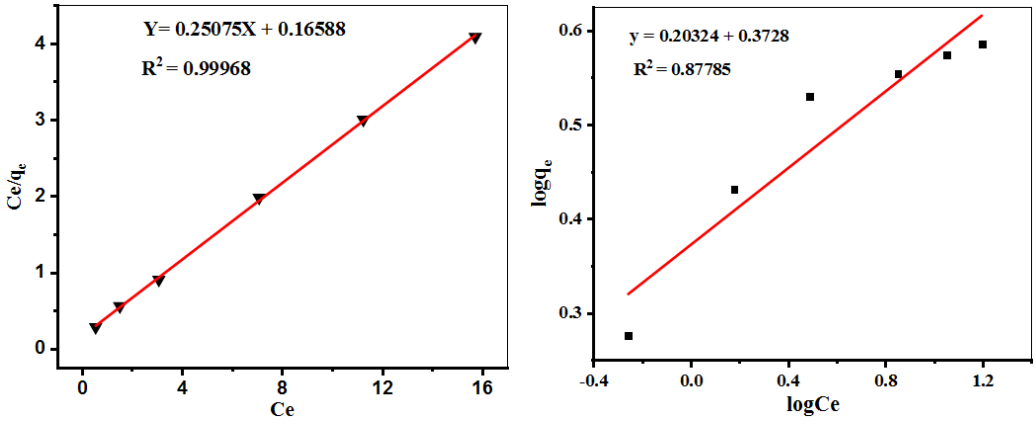

(a) (b)

Figure 13. *Langmuir adsorption (a) and Freundlich adsorption (b) isotherm studies for AC of LA.*

Otherwise, desorption becomes predominant. If n = 1, the adsorption is linear. For n <1, the adsorption is chemisorption and for n >1 the adsorption is favorable physical adsorption (Tadesse, 2019). As we can observe from Figure 9b, Figure 9c, and Table 2, the adsorption of MB on LA is best fitted with the Langmuir isotherm.

Table 2. *Langmuir and Freundlich Adsorption Isotherm Constants for the Adsorption of MB on AC of LA.*

Isothermal line model	Parameters	Results
Langmuir	K_L (L/mg)	1.511

Isothermal line model	Parameters	Results
	q_{max} (mg/g)	3.99
	R^2	0.999
	R_L	0.062 to 0.0186
Freundlich	K_F(mg/g).(mg/L) $^{\frac{1}{n}}$	2.36
	N	4.921
	R^2	0.87785

3.6. Adsorption Kinetic Study

Kinetic models have been utilized to analyze experimental data to understand the adsorption mechanism and identify potential rate control steps such as mass transfer and chemical reaction. The adsorption kinetics, which represent the solute removal rate governing the residence time of the sorbent at the solid-solution interface, are summarized in Table S11. These models encompass pseudo-first-order and pseudo-second-order models [55].

Pseudo First & Second Order Adsorption Kinetics

The Lagergen pseudo-first-order equation [56], is generally expressed as follows:

$$\log\frac{q_e}{q_e-q_t} = \frac{k_1}{2.303}t \quad (13)$$

Where, q_e and q_t refer to the amount of dye adsorbed (mg g^{-1}) at equilibrium and at any time, t (min), respectively, and k1 is the equilibrium rate constant of the pseudo-first-order sorption (min^{-1}). After integration and applying boundary conditions, t = 0 and t=t and q_t=0 to q_t=q_t. the integrated form of Eq. (13) becomes:

$$\log(q_e - q_t) = \log q_e - \frac{k_1}{2.303}t \quad (14)$$

The values of k_1 and q_e were calculated from the slopes and intercepts of log (q_e-q_t) against the plots t. The pseudo first-order plot of MB adsorption on LA shown in Figure 4a. The equation corresponding to the pseudo-second-order kinetic model is the following:

$$\frac{1}{q_e-q_t} = \frac{1}{q_e} + k_2 t \quad (15)$$

The linearized integral form of this model is (the Lagergen pseudo- second order kinetic model) given as:

$$\frac{t}{q_t} = \frac{1}{k_2 q_e^2} + \frac{1}{q_e}t \quad (16)$$

where k_2 is the rate constant of second-order adsorption (g/mg/min). Slope and intercept of plot of t/q_t against t, give values of q_e and K2, respectively, Figure 14b. As can be viewed in Table 3 for AC made from LA, the result showed a very good compliance with the pseudo-second order equation with high regression coefficients (R^2) compared with pseudo-first order.

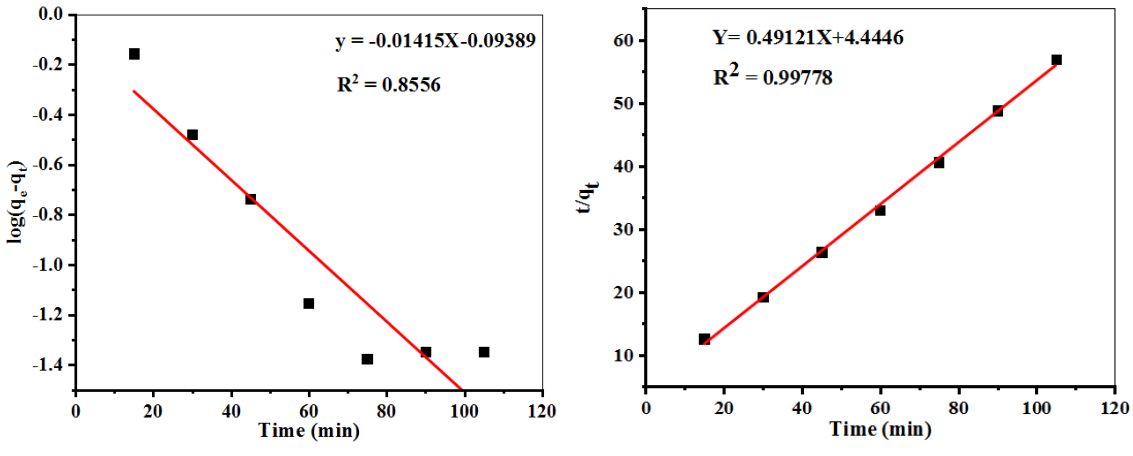

(a) (b)

Figure 14. *Pseudo First–order kinetics (a) and Pseudo Second–order kinetics (b) for adsorption for adsorption of MB on AC of LA.*

Table 3. Pseudo-first and pseudo-second order kinetic model constants for the adsorption of MB on AC of LA.

Kinetics model	Parameters	Results
Pseudo First–order	q_e(cal.)	0.806
	q_e(exp.)	1.89
	k_1	0.033
	R^2	0.856
Pseudo Second–order	q_e(cal.)	2.0
	q_e(exp.)	1.89
	k_2	0.054
	R^2	0.998

3.7. Comparison of Previously Reported Adsorption Capacity with Different Adsorbents for MB Removal

The adsorption capacity of the adsorbent for the adsorption of MB has been comparable with those of others reported in the literature and the values of adsorption capacity as presented in Table 4. The experimental data of the present investigation were compared with the values reported. The result of our investigation revealed that LA-Ac has the highest percent adsorption and adsorption capacity.

Table 4. Previously reported adsorption capacities of various a sorbents for methylene blue.

Adsorbent	q_{max} (mg/g)	Reference
Kaolin	1.63	[57]
Biochar-palm bark	2.66	[58]
Biochar eucalyptus	2.06	[58]
Black Tea Wastes	3.367	[18]
Grape leaves	0.2	[21]
Arundinaria Alpina	2.49	[34]
Koseret leaves	3.99	(This study)

4. Conclusions

The aim of this study is to synthesize and characterize new biomaterial-derived activated carbon (AC) from *Lippia Adoensis leaf* (Koseret) (LA) by chemical activation with H_3PO_4 and evaluate its performance for the application of MB removal. The AC of the LA leaf was characterized by FTIR, SEM, iodine number, and MB number. The result of the characterization showed that LA has a well-developed surface area for adsorption. From the iodine number, the prepared AC of LA shows the highest macroporous surface area. The surface functional group was investigated by FT-IR spectroscopy techniques. pHpzc showed that activated carbon has a slightly acidic surface functional group. The data from batch experiments indicated that the adsorption of MB by LA leaf AC depends on various parameters such as pH, dosage, contact time, and initial concentration of MB. Optimal dose values = 0.25 g, pH = 8, initial concentration of MB = 10 ppm and contact time = 75 min were observed. The data obtained from the thermodynamic parameters, with the results indicating a negative value of ΔG°, suggested that the adsorption was spontaneous in nature. The positive values of ΔH^0 and ΔS^0 indicated endothermic adsorption processes and increased randomness at the surface-solution interface, respectively. The Langmuir model showed the best fit to the adsorption data (R^2 = 0.999), and the kinetic data followed a pseudo-second order model, which was confirmed. Finally, the results show that the AC of LA could be economically achievable for the removal of MB from an aqueous solution. Even if tested for MB only, one can carefully assume that AC of LA will present similar adsorption performances for the elimination of multiple organic dyes from aqueous solutions.

Abbreviations

AC	Activated Carbon
LA	*Lippia Adoensis*
LA-AC	*Lippia Adoensis*- Activated Carbon
MB	Methylene Blue
SEM	Scanning Electron Microscope
FT-IR	Fourier Transform Infrared Spectroscopy
ΔG^0	Gibbs Free Energy
ΔS^0	Entropy
ΔH^0	Enthalpy

Supplementary Material

The supplementary material can be accessed at https://doi.org/10.11648/j.ajac.20241202.11

Acknowledgments

We thank Hawassa University, Department of Chemistry, for providing laboratory facilities such as instruments and chemical support during laboratory analysis.

Author Contributions

Mesesle Mengesha: Conceptualization, Writing original draft, Design and conception of experiments, Collect data, Validation Investigation and formal analysis, Project administration

Yohannes Shuka: Conceptualization, Methodology; Analyzed and interpreted the data; Resources, analysis tools and software; Validation, Writing – review & editing and Supervision, Visualization

Tesfahun Eyoel: Writing – review & editing, Investigation, formal analysis

Tekalign Tesfaye: Analysis tools or data; Validation, Writing – review & editing, Acquisition of funds

Data Availability Statement

The data and material used to support the findings of this study are available in the SI, and additional information is available from the corresponding author upon request.

Conflicts of Interest

The authors declare no conflicts of interest.

References

[1] Jara, Y. S., Mekiso, T. T. & Washe, A. P. Highly efficient catalytic degradation of organic dyes using iron nanoparticles synthesized with Vernonia Amygdalina leaf extract. *Sci Rep* (2024), 14, 6997. https://doi.org/10.1038/s41598-024-57554-5

[2] Ramutshatsha-Makhwedzha, D., Mavhungu, A., Moropeng, M. L., & Mbaya, R.. Activated carbon derived from waste orange and lemon peels for the adsorption of methyl orange and methylene blue dyes from wastewater. *Heliyon*, (2022) 8, 1–9. https://doi.org/10.1016/j.heliyon.2022.e09930

[3] Al-Mokhalelati, K., Al-Bakri, I., & Al Shibeh Al Wattar, N. Adsorption of methylene blue onto sugarcane bagasse-based adsorbent materials. *Journal of Physical Organic Chemistry*, (2021) 34(7). https://doi.org/10.1002/poc.4193

[4] Goswami, L., Kushwaha, A., Kafle, S. R., & Kim, B. S. Surface modification of biochar for dye removal from wastewater. Catalysts, (2022) 12(8), 817. https://doi.org/10.3390/catal12080817

[5] Zewde, D., & Geremew, B.. Removal of Congo red using Vernonia amygdalina leaf powder: optimization, isotherms, kinetics, and thermodynamics studies. *Environmental Pollutants and Bioavailability*, (2022) 34(1), 88–101. https://doi.org/10.1080/26395940.2022.2051751

[6] Gayathiri, E., Prakash, P., Selvam, K., Awasthi, K., Gobinath, R., Karri, R. R., Ragunathan, G., Jayanthi, J., & Mani, V. Plant microbe based remediation approaches in dye removal: A review. Bioengineered, (2022) 13(3), 7798–7828. https://doi.org/10.1080/21655979.2022.2049100

[7] Mousavi, S. A., Mehralian,., Khashij, M., & Parvaneh, S. Methylene blue removal from aqueous solutions by activated carbon prepared from N. Microphyllum (AC-NM): RSM analysis, isotherms and kinetic studies. *Glob. Nest J.*, (2017) 19(4), 697–705. https://doi.org/10.30955/gnj.002422

[8] Moharm, A. E., El Naeem, G. A., Soliman, H. M. A., Abd-Elhamid, A. I., El Bardan, A. A., Kassem, T. S., Nayl, A. A., & Bräse, S. Fabrication and Characterization of Effective Biochar Biosorbent Derived from Agricultural Waste to Remove Cationic Dyes from Wastewater. *Polymers*, (2022) 14(13), 1–16. https://doi.org/10.3390/polym14132587

[9] Aaga, G. F., & Anshebo, S. T. Green synthesis of highly efficient and stable copper oxide nanoparticles using an aqueous seed extract of Moringa stenopetala for sunlight-assisted catalytic degradation of Congo red and alizarin red s. *Heliyon*, (2023) 9(5).

[10] Robles-Melchor, L., Cornejo-Mazon, M., Hernian-dez-Martinez, D. M., Gustavo F. Gutierrez-Lopez, Gustavo F., Garcia-Pinilla, S., Lopez-Villegas, E. O., & Tellez-Medina, D. I.. Removal of Methylene Blue from Aqueous Solutions by Using Nance (Byrsonima crassifolia) Seeds and Peels as Natural Biosorbents. *Journal of Chemistry*, (2021)1–13. https://doi.org/10.1155/2021/5556940

[11] Modi, S., Yadav, V. K., Gacem, A., Ali, I. H., Dave, D., Khan, S. H., Yadav, K. K., Rather, S., Ahn, Y., & Son, C. T. Recent and Emerging Trends in Remediation of Methylene Blue Dye from Wastewater by Using Zinc Oxide Nanoparticles. *Water*, (2022) 14(1749), 2–26. https://doi.org/10.3390/w14111749

[12] Al-Maliky, E. A., Gzar, H. A., & Al-Azawy, M. G.. Determination of Point of Zero Charge (PZC) of Concrete Particles Adsorbents. IOP Conference Series: *Materials Science and Engineering*, (2021) 1184(1). https://doi.org/10.1088/1757-899x/1184/1/012004

[13] Kaykhaii, M., Sasani, M., and Marghzari, S. Removal of Dyes from the Environment by Adsorption Process. (2018) 6(2), 31–35. https://doi.org/10.13189/cme.2018.060201

[14] Sharma, S., & Kaur, A. Various methods for removal of dyes from industrial effluents - a review. *Indian Journal of Science and Technology*, (2018) 11(12), 1–21. https://doi.org/10.17485/ijst/2018/v11i12/120847

[15] Ikram, M.; Naeem, M., Zahoor, M., Hanafiah, M. M., Oyekanmi, A. A., Ullah, R., Farraj, D. A. A., Elshikh, M. S., Zekker, I., & Gulfam, N. Biological Degradation of the Azo Dye Basic Orange 2 by Escherichia coli: A Sustainable and Ecofriendly Approach for the Treatment of Textile Wastewater. *Water* (Switzerland), (2022) 14(13). https://doi.org/10.3390/w14132063

[16] Samsami, S., Mohamadi, M., Rene, E. R., & Firoozbahr, M. Recent advances in the treatment of dye-containing wastewater from textile industries: Overview and perspectives. Process of Saf. Environmental Protection, (2020). https://doi.org/10.1016/j.psep.2020.05.034

[17] Deng, H., Lu, J., Li, G., Zhang, G., and Wang, X. Adsorption of methylene blue on adsorbent materials produced from cotton stalk. *Chemical Engneering Journl*, (2011) 172(1), 326–334. https://doi.org/10.1016/j.cej.2011.06.013

[18] Ullah, A., Zahoor, M., Din, W. U., Muhammad, M., Khan, F. A., Sohail, A., Ullah, R., Ali, E. A., & Murthy, H. C. A.. Removal of Methylene Blue from Aqueous Solution Using Black Tea Wastes: Used as Efficient Adsorbent. *Adsorption Science and Technology*, (2022)1–9. https://doi.org/10.1155/2022/5713077

[19] Cheng, J., Zhan, C., Wu, J., Cui, Z., Si, J., Wang, Q., Xiangfang Peng, X., & Turng, L. Highly Efficient Removal of Methylene Blue Dye from an Aqueous Solution Using Cellulose Acetate Nanofibrous Membranes Modified by Polydopamine. *ACS Omega*, (2020) 5(10) 5389–5400. https://doi.org/10.1021/acsomega.9b04425

[20] Malatji, N., Makhado, E., Modibane, K. D., Ramohlola, K. E., Maponya, T. C., Monama, G. R., & Hato, M. JRemoval of methylene blue from wastewater using hydrogel nanocomposites. *A review*, (2021) 11, 1–27. https://doi.org/10.1177/18479804211039425

[21] Mousavi, S. A., Mahmoudi, A., Amiri, S., Darvishi, P., & Noori, E. Methylene blue removal using grape leaves waste: optimization and modeling. *Applied Water Science*, (2022) 12(5), 1–11. https://doi.org/10.1007/s13201-022-01648-w

[22] Das, M., & Mishra, C. Jackfruit leaf as an adsorbent of malachite green: recovery and reuse of the dye. *SN Applied Science*, (2019) 1(5). https://doi.org/10.1007/s42452-019-0459-7

[23] Bhattacharyya, K. G., & Sharma, A. Kinetics and thermodynamics of Methylene Blue adsorption on Neem (*Azadirachta indica*) leaf powder. (2005) 65, https://doi.org/10.1016/j.dyepig.2004.06.016

[24] S ánchez-Orozco, R., Mart ínez-Juan, M., Garc á-S ánchez, J. J., & Ure ña-N úñez, F. Removal of methylene blue from aqueous solution using Typha stems and leaves. *BioResources*, (2018) 13(1), 1696–1710. https://doi.org/10.15376/biores.13.1.1696-1710

[25] Mosoarca, G., Popa, S., C. Vancea, C., Dan, M., & Boran, S. Removal of Methylene Blue from Aqueous Solutions Using a New Natural Lignocellulosic Adsorbent—Raspberry (Rubus idaeus) Leaves Powder. *Polymers (Basel)*, (2022) 14(10). https://doi.org/10.3390/polym14101966

[26] Journal, A. P & Consortium, A. B. Evaluation of Antibacterial Activity and Phytochemical Constituents of Leaf Extract of Lippia adoensis. *Asia Pacific Journal Energy Environment*, (2014) 1(1), 43–55.

[27] Buli, G. A., Duga, A. G., & Dessalegn, E. Antimicrobial Activity of Lippia adoensis var. koseret Against Human Pathogenic Bacteria and Fungi. *American Journal of Clinical and Experimental Medicine* (2015) 3(3), 118–123. https://doi.org/10.11648/j.ajcem.20150303.18

[28] Datu, Kinniso Genemo. "Antioxidant and antimicrobial potentials of endophytic fungifrom (lippia adoensis hoechst. var. koseret) leaf and seed." PhD diss., Haramaya University, 2023.

[29] Belachew G, Engeda D, Tilku D. In vitro antioxidant activity of Lippia adoensis Var. Koseret, Thymus schimperi Ronniger and Rosmarinus officinalis Leaf extracts and their effects on oxidative stability of ground raw beef meat during refrigeration storage. *Food Res*. (2022) 6(5): 319-27. https://doi.org/10.26656/fr.2017.6(5).830

[30] Hashemian S, Salari K, Yazdi ZA. Preparation of activated carbon from agricultural wastes (almond shell and orange peel) for adsorption of 2-pic from aqueous solution. *Journal of Industrial and Engineering Chemistry*. (2014) Jul 25; 0(4): 892-900. https://doi.org/10.1016/j.jiec.2013.09.009

[31] Örkün, Y., N. Karatepe, and R. Yavuz. "Influence of Temperature and Impregnation Ratio of H_3PO_4 on the Production of Activated Carbon from Hazelnut Shell." *Acta Physica Polonica A 121, no. 1*(2012): 277-280.

[32] Juzsakova, T., Salman, A. D., Abdullah, T. A., Rasheed, R. T., Zsirka, B., Al-Shaikhly, R. R., & Sluser, B. Removal of Methylene Blue from Aqueous Solution by Mixture of Reused Silica Gel Desiccant and Natural Sand or Eggshell Waste. *Materials (Basel)*, (2023) 16(4), 1–23. https://doi.org/10.3390/ma16041618

[33] Ghazi Mokri, H. S., Modirshahla, N., Behnajady, M. A., & Vahid, B. Adsorption of C. I. Acid Red 97 dye from aqueous solution onto walnut shell. kinetics, thermodynamics parameters, isotherms. *International Journal of Environmental Science and Technology*, (2015) 12(4), 1401–1408. https://doi.org/10.1007/s13762-014-0725-6

[34] Tadesse, S. Removal of Basic Dye from Aqueous Medium Using Activated Carbon from Erythrina Brucei, Arundinaria Alpina and Manihot Esculenta. *Food Science and Quality Management*, (2019) 86, 19–27. https://doi.org/10.7176/fsqm/86-03

[35] Kaya, M., Azahin, O., & Saka, C. Preparation and TG/DTG, FT-IR, SEM, BET Surface Area, Iodine Number and Methylene Blue Number Analysis of Activated Carbon from Pistachio Shells by Chemical Activation. *International Journal of Chemical Reactor Engineering*, (2018) 16(2), 1–13. https://doi.org/10.1515/ijcre-2017-0060

[36] Nunes, C. A., & Guerreiro, M. C. Estimation of surface area and pore volume of activated carbons by methylene blue and iodine numbers. *Quimica Nova*, (2011) 34(3), 472–476. https://doi.org/10.1590/S0100-40422011000300020

[37] Ekpete, O. A., Marcus, A. C., & Osi, V. Preparation and Characterization of Activated Carbon Obtained from Plantain (Musa paradisiaca) Fruit Stem. *Jourinal of Chemistry*, (2017). https://doi.org/10.1155/2017/8635615

[38] Bhavsar, P. A., Jagadale, M. H., Khandetod, Y. P., & Mohod, A. G. Proximate Aalysis of Selected Non Woody Biomass. *International Journal of Current Microbiology and Applied Sciences*, (2018) 7(09), 2846–2849. https://doi.org/10.20546/ijcmas.2018.709.353

[39] Solomon, O., Kayode, B., Adegoke, A., & Omowumi, OPreparation and characterization of a novel adsorbent from Moringa oleifera leaf. *Applied Water Science*, (2017) 7(3), 1295–1305. https://doi.org/10.1007/s13201-015-0345-4

[40] Ishaku, A. A., Asheofo, D., Habibu, T., Sunday, T. M., Amuta, E. A., & Azua, A. T. Prevalence of intestinal parasitic infections among food vendors in Lafia Metropolis of Nasarawa State, *Nigeria*. (2013) 2(2), 21–25.

[41] Afroze, S. & Kanti, T. Adsorption performance of continuous fixed bed column for the removal of methylene blue (MB) dye using Eucalyptus sheathiana bark biomass. *Research on Chemical Intermediates*, (2016) 42, 2343–2364. https://doi.org/10.1007/s11164-015-2153-8

[42] Pandiangan, K. D., Arief, S., Jamarun, N., & Simanjuntak, W. Synthesis of zeolite-X from rice husk silica and aluminum metal as a catalyst for transesterification of palm oil. *Journal of Materials and Environmental Science*, (2017) 8(5), 1797-1802.

[43] Boukhemkhem, A., & Rida, K. Improvement adsorption capacity of methylene blue onto modified Tamazert kaolin. *Adsorption Science & Technology*, (2017) 35(9-10), 753-773. https://doi.org/10.1177/0263617416684835

[44] Sani, T., Gómez-hortigüela, L., Pérez-pariente, J., Chebude, Y., & Díaz, I. Defluoridation performance of nano-hydroxyapatite / stilbite composite compared with bone char. *Separation and purification technology*, (2015) 157(8), 241–248. https://doi.org/10.1016/j.seppur.2015.11.014

[45] Salunkhe, B. & Schuman, T. P. Super-Adsorbent Hydrogels for Removal of Methylene Blue from Aqueous Solution: Dye Adsorption Isotherms, Kinetics, and Thermodynamic Properties. *Macromol*, (2021) 1(4), 256–275. https://doi.org/10.3390/macromol1040018

[46] Dawood, S & Sen, T. K. Review on Dye Removal from Its Aqueous Solution into Alternative Cost Ef-fective and Non-Conventional Adsorbents. *Journal of Chemical and Process Engineering*, (2014) 1(104), 1–11.

[47] Zhou, Y., Ge, L., & Fan, F. Adsorption of Congo red from aqueous solution onto shrimp shell powder. *Adsorption Science and Technology*, (2018) 1–21. https://doi.org/10.1177/0263617418768945

[48] Salleh, M. A. M., Mahmoud, D. K., Karim, W. A. W. A., & Idris, A. Cationic and anionic dye adsorption by agricultural solid wastes: A comprehensive review. *Desalination*, (2011) 280(3), 1–13. https://doi.org/10.1016/j.desal.2011.07.019

[49] Yagub, M. T., Sen, T. K. Afroze, S., & Ang, H. M. Dye and its removal from aqueous solution by adsorption: A review. *Advances in Colloid and Interface Science*, (2014) 209. 172–184, https://doi.org/10.1016/j.cis.2014.04.002

[50] Gebeyehu, B. T., Kabtamu, D. M., & Tasew, T. A. Efficient removal of methylene blue dye from aqueous solution using a new biosorbent derived from Ensete ventricosum (Enset). *Bulletin of the Chemical Society of Ethiopia*, (2024) 38(1), 69-84. https://doi.org/10.4314/bcse.v38i1.6

[51] Roy, A., Chakraborty, S., Kundu, S. P. Adhikari, B., & Majumder, S. B. Adsorption of anionic-azo dye from aqueous solution by lignocellulose- biomass jute fiber: Equilibrium, kinetics, and thermodynamics study. *Industrial and Engineering Chemistry Research*, (2012) 51(37), 12095–12106. https://doi.org/10.1021/ie301708e

[52] Demirbas, A. Agricultural based activated carbons for the removal of dyes from aqueous solutions: A review. *Journal of Hazardous Materials*, (2009) 167(3), 1–9. https://doi.org/10.1016/j.jhazmat.2008.12.114

[53] Kavitha, G., P. Subhapriya, Dhanapal, V., Dineshkumar, G., & Venkateswaran, V. Dye removal kinetics and adsorption studies of activated carbon derived from the stems of Phyllanthus reticulatus. *Materials Today: Proceedings*, (2021) 45, 7934–7938, https://doi.org/10.1016/j.matpr.2020.12.837

[54] Krishni, R. R., Foo, K. Y., & Hameed, B. H. Adsorptive removal of methylene blue using the natural adsorbent-banana leaves. *Desalination and Water Treatment*, (2014) 52(31), 6104–6112. https://doi.org/10.1080/19443994.2013.815687

[55] Ahmad, M. A. & Alrozi, R. Removal of malachite green dye from aqueous solution using rambutan peel-based activated carbon: Equilibrium, kinetic and thermodynamic studies. *Chemical Engineering Journal*, (2011) 171(2), 510–516. https://doi.org/10.1016/j.cej.2011.04.018

[56] Gómez, V., Larrechi, M. S., & Callao, M. P. Kinetic and adsorption study of acid dye removal using activated carbon. *Chemosphere*, (2007) 69(7), 1151–1158. https://doi.org/10.1016/j.chemosphere.2007.03.076

[57] Zemedkun, M., Tagesse, D. W., & Yihunie, A. Removal of methylene blue from textile waste water using kaolin and zeolite-x synthesized from Ethiopian kaolin. *Environmental Health and Toxicology: EHT*, (2021) 36(1), 7-7. https://doi.org/10.5620/eaht.2021007

[58] Sun, L., Wan, S., & Luo, W. Biochars prepared from anaerobic digestion residue, palm bark, and eucalyptus for adsorption of cationic methylene blue dye: Characterization, equilibrium, and kinetic studies. *Bioresource Technology*, (2013) 140, 406–413. https://doi.org/10.1016/j.biortech.2013.04.116

Biography

Mesele Mengesha is a lecturer at Chemistry Department of Wolaita Soddo University, Ethiopia. He acquired his MSc in Physical Chemistry from Hawassa University in 2023. He has participated in multiple national and international research collaboration projects in recent years. He currently serves on the Green Chemistry coordinator of WSU in National Green legacy project and peer reviewer member of a publications.

Yohannes Shuka is a laboratory analyst, and younger researcher and Lecturer, in the Chemistry Department at Madda Walabu University, Ethiopia. He graduated with honors from Dilla University with a BSc in Applied Chemistry in 2019. He earned his MSc in Physical Chemistry from Hawassa University in 2024. In recent years, he has been actively involved in various national and international research collaborations and projects. He has authored five publications in related fields, written one book, and developed three laboratory manuals. He is also a reviewer and peer reviewer for two scientific journals.

Tesfahun Eyoel is a lecturer and researcher at Chemistry Department of Wolaita Soddo University, Ethiopia. He acquired his MSc in Physical Chemistry from Hawassa University in 2023 He has participated in multiple national and international research collaboration projects in recent years. He currently serves on the reviewer of WSU Journal and publications.

Tekalign Tesfaye is a lecturer at Chemistry Department of Mettu University, Ethiopia. He acquired his MSc in Physical Chemistry from Hawassa University in 2023. He has participated in multiple national and international research collaboration projects in recent years. He currently serves on the Green Chemistry coordinator of Mettu in National Green legacy project and young researcher at MFC green energy production.

Research Field

Mesele Mengesha: Environmental remediation, Green chemistry, Adsorption, Biosorbent

Yohannes Shuka: Nano-catalyst design, Nano particle and nano technology, Green energy, Photocatalysis, Detoxification, Bio sensing Materials

Tesfahun Eyoel: Catalysis, Photocatalysis, Bio-Photoctalysis, Nanoparticles

Tekalign Tesfaye: Nano particle and nano technology, Green energy, Electrochemistry, Bio sensing Materials